Journal of Physical Science, Vol. 29(2), 89–112, 2018

A New Treatment to Compute the Track Parameters in PADC Detector using Track Opening Measurement

Saeed Hassan Al-Nia'emi

Physics Department, College of Education for Pure Science,
University of Mosul, 00964 Iraq

e-mail: saeed_alnaeme@yahoo.com

Published online: 25 August 2018

To cite this article: Al-Nia'emi, S. H. (2018). A new treatment to compute the track parameters in PADC detector using track opening measurement. *J. Phys. Sci.*, 29(2), 89–112, https://doi.org/10.21315/jps2018.29.2.6

To link to this article: https://doi.org/10.21315/jps2018.29.2.6

ABSTRACT: *In this paper, a new treatment or method has been presented to calculate the parameters of the etched track and its shape development after irradiating polyallyldiglycol carbonate (PADC) detector CR-39 by alpha particles using direct measurement of the track opening diameters. The method is based on a concept that the track diameter growth rate (V_D) and the track etch rate (V_T) are not constants with the progressing of the etching process. Some of the equations used in the case of V_D to be a constant have been modified as a function of etching time to be more suitable for the case. Certain boundary conditions have been extracted from previous works based on the measurement of the track lengths directly from the track's images, to use them in the equations that were applied to figure out the track parameters in the present work. A CR-39 detector was irradiated with alpha particles having energies of 1.53 MeV, 2.35 MeV, 3.06 MeV, 3.80 MeV and 4.44 MeV under normal incidence using 1 μCi ^{241}Am source of 5.485 MeV. The irradiated detectors were etched chemically with an aqueous 6.25 N solution of NaOH at 70°C. The track parameters and the profile development, as well as the V(R') function, were determined. The results obtained by this method using the track diameters information showed a good agreement with previous works that used the direct measurement of the track lengths*

Keywords: Solid-state nuclear track detector, PADC, track growth, CR-39, V function

1. INTRODUCTION

In the solid state nuclear detector (SSNTD), the study of charged particle tracks (etch-pits) geometry by experimental methods using direct imaging of the track profiles, and analytical methods using certain computer programs to draw the

track profiles, have became a great importance to understand the track growth in different phases of development.[1–12] The mechanism of the track growth in the SSNTD is not an arbitrary process, but it can be organised by controlling the two main parameters: the bulk etch rate (V_B) of the detector surface, and the track etch rate (V_T) along the particle path in the detector. Therefore, many studies have been carried out to understand the mechanism of the track geometry (track lengths, depths and other track parameters) in several solid-state nuclear detectors such as the polycarbonate CR-39 and cellulose nitrate LR-115.[13–18]

The imaging of the track profiles (walls and openings) during the etching process for measuring their lengths and calculating other parameters rather than the use of the direct measurement of their diameter openings, has received a considerable attention by researchers in this field. Different imaging methods were employed to image the etched tracks and measure their lengths (depths) in the CR-39 detector. In these methods, the techniques used are: (1) the replica technique which is based on measuring the replica height (track length);[19,20] (2) breaking the etched detector perpendicular to its surface and then polishing its edge to focus the lateral image and longitudinal cross-section of the track profiles;[21,22] and (3) using the confocal microscope to image the track shape.[16,23,24] Recently, in most of our works we have been using an easier imaging way by irradiating the side (edge) of the detector with alpha particles (lateral irradiation method) and then focusing vertically the longitudinal etched tracks from the surface of the detector using an ordinary optical microscope connected to a computer through a digital camera.[15,17,18,25]

It has been found that the direct measurement of the track length by image method gives accurate outcomes in calculating the track parameters better than that obtained from the traditional measurements of the track openings. Thus, the direct measurement of the track length contributes to determining the real changes of V_T which is dialectically related to the changes of the track walls and the openings of the etched pits with the etching advancement. The change in V_T, in turn, will give the change in the etch rate ratio (V) related to V_B as $V = V_T/V_B$, where V_B is usually constant.[7,8,16,26] Therefore, this kind of measurements provided a precise understanding of the etched track formation and evolution stages during the advancing of the etching action.

The measuring of the track profile with its length and the other calculated parameters in the two phases of track development, the acute conical and over-etched phases have attracted much attention in recent years.[8,11] The first phase extends from the original surface along the damaged region up to the end of the particle trajectory in the detector (i.e., for $x \leq R$), while the second phase starts from the end of the particle trajectory beneath the track tip in the undamaged region for $x > R$.[4,5]

Here, x is the depth of the track tip from the original surface of the detector, and R is the particle range in the detector.

In this paper, it was noted that the relationship between the track diameters of the alpha particles and the etching time is an exponential change, which results in a little bit of variety in the track diameter growth rate (V_D). As a new or alternative method, the time dependent of V_D was considered to determine the real change and development of the track profiles in the PADC CR-39 detector and to compute the track length and other parameters using the direct measurement of the track diameters instead of the direct measurement of the track image lengths.

2. CALCULATIONS AND THE BOUNDARY CONDITIONS

The new treatment suggests a modification in some of the equations that assume a constancy in V_D and change in the V_T with the etching time for calculating the track parameters. The treatment process has required certain empirical boundary conditions, which we have extracted from the results based on the direct measurement of the track lengths.[8,15,17,18,26] These conditions are adapted to apply the modified equations to calculate the track parameters using the information obtained from the direct measurement of the track diameters in order to get results coincidence with that obtained by the direct measurements of the track lengths.

For the values of V_D and V_T are not constants, and V_B is usually constant, the equations can be modified or adjusted as the following descriptions.

When V_D is not constant with the etching time, it can be expressed as a time dependent function as:

$$V_D(t) = \frac{dD(t)}{dt} = \text{slope}(t) \tag{1}$$

This formula represents the slope of the experimental D-t curve at any point or etching time. Accordingly, the equation of V_D given by Durrani and Bull can be written in the form of a function of time:[27]

$$V_D(t) = 2V_B\sqrt{\frac{V-1}{V+1}} \tag{2}$$

For V_T is not constant with the etching time, the track length growth rate is given as:[28,29]

$$\frac{dL(t)}{dt} = V_T(t) - V_B \tag{3}$$

and the etch rate ratio is:

$$V = \frac{V_T(t)}{V_B} \tag{4}$$

Combining Equations 2, 3 and 4, the track length growth rate can be expressed as:

$$L'(t) = \frac{2V_B}{k^2 - 1} \tag{5}$$

where

$$L'(t) = \frac{dL(t)}{dt} \tag{5a}$$

and

$$k = \left(\frac{2V_B}{V_D(t)}\right) \tag{5b}$$

To compute the track length, one can utilise the integration below:

$$L(t) = \int_0^t L'(t)dt \tag{6}$$

The track depth (x), which represents the depth from the original surface of the detector to the track tip at a certain etching time, is calculated from the known relationship:[27]

$$x(t) = \int V_T(t)dt = L(t) + V_B t \tag{7}$$

Also, the residual range R'(t) of the charged particle is:[6,8]

$$R'(t) = R - x(t) \tag{8}$$

where R is the range of the charged particle in the detector, and it is the particle energy dependent.

Regarding the previous equations, the boundary conditions assume that the etching solution reaches the end of the particle range in the detector, then the track depth will be equal to the particle range (i.e., x = R) and the residual range approach to zero (R' = 0). Therefore, the boundary conditions can be expressed as follows:

1. When R' is close to zero at the Bragg-peak; the conical phase:

   $L'(t) = \frac{dL(t)}{dt} = \max, V_T = \max, V = \max$

2. When R' = 0, x = R; the conical phase where the track is etched-out:

$L(t) = L_{max}$ = const. (saturation point) and $L'(t) = \frac{dL(t)}{dt} = 0$,

$V_T \rightarrow V_B$ and $V \rightarrow 1$

3. When x > R, R' = -ve; the over-etched phase:

$L(t) = L_{max}$ = const. (saturation) and $L'(t) = \frac{dL(t)}{dt} = 0$, $V_T = V_B$ and $V = 1$

3. METHODOLOGY

In the present study, PADC detector CR-39 with thickness 250 μm from Page Mouldings (Worcestershire, England) was cut into several pieces with sizes of 1.5 × 1.5 cm^2. The detector pieces were irradiated by alpha particles with energies of 1.53 MeV, 2.35 MeV, 3.06 MeV, 3.80 MeV and 4.44 MeV under normal incidence. A 1 μCi ^{241}Am source with main energy 5.485 MeV was used in irradiation. The energy of the alpha particle was varied by changing the source to detector distance in air under atmospheric pressure. The irradiated detectors were chemically etched in an aqueous 6.25N NaOH solution at 70°C ± 1°C for different periods of time according to the alpha particle energies, and the track diameters were then measured. It should be noted that the diameter measured in each etching period represents the average diameter of about 100–120 tracks with a percentage error about 5%–6%.

The method based on the thickness difference before and after the etching process was used in the determination of V_B. The CR-39 detector of the same dimensions as mentioned was etched under the same etching conditions for a successive interval of 0.5 h up to 8 h. The thickness of the removed layer (h) from the surface of the detector was extracted for each period of etching (t). The V_B is then calculated by using the relation below:

$$V_B = \Delta h / \Delta t \quad (\text{in } \mu m\ h^{-1}) \tag{9}$$

The track diameters and the detector thickness were measured by utilising the optical microscope (XSZ-H Series Biological Microscope) connected to a PC through a digital camera (MDCE-5A).

4. RESULTS AND DISCUSSION

4.1 Track Diameter

Figure 1 illustrates the relationship between the track diameter of the alpha particle and the etching time in the CR-39 detector at the energy range of 1.53–4.44 MeV. The figure shows that the relationship is relatively nonlinear, particularly with the advancing of the etching operation. Although the relationship is close to the linear form, we have employed the polynomial function of degree two in the figure to obtain a nonlinear relationship between the track diameters and the etching times. The nonlinear relationship is resulting in the track diameter growth rate to be a time dependent ($V_D(t)$) rather than the linear one, which gives a constant V_D for a single energy of the alpha particles. However, calculations based on the direct measurement of the track diameters with constant V_D cannot recognise the real changes of the track profiles and parameters as those found from the direct measurement of the track length.

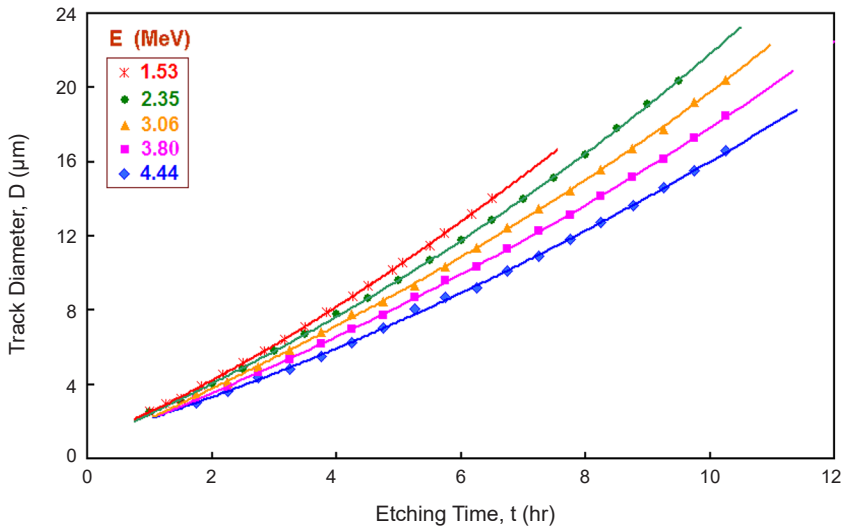

Figure 1: Relationship between the track diameter and etching time for different alpha particle energies in CR-39.

The little bit nonlinearity change in the track diameters agreed with findings by Azooz et al.[11,18] It can be clearly observed that the nonlinear increase in the track diameter at etching periods is more than the time of reaching the etchant to the end of the particle range, especially when the track tip enters the undamaged region (over-etched phase).

It ought to be mentioned that the potential energy of the damaged regions produced by alpha particles with low energies is higher than the damaged regions created by high energies. Accordingly, V_T will be higher in the regions with a high potential energy, prompting formation of etched tracks with a size bigger than other regions having low potential energies as appeared in Figure 1.

4.2 Track Diameter Growth Rate (V_D)

Using differential calculus, V_D as a function of the etching time, $V_D(t)$ was obtained (according to the Equation 1) by determining the slope (dD(t)/dt) of the D-t curves in Figure 1 at experimentally used etching times as well as at the other selected times within the range of the etching period. The variation of V_D values with the etching time is obviously seen in Figure 2. It can be seen from the figure that V_D is proportional to the etching time and it increases with the advancing of the etching operation. This result appeared in good agreement with that found by Roussetski et al. in alpha particle irradiated CR-39 detector for energies between 10–13 MeV and 15–17.5 MeV.[30]

As a result, we can find that the V_D is not constant, but it changes with the etching time and has different values rather than single definite one for each individual energy of alpha particle irradiation. This result represents the concept of this study which is based on the modified equations.

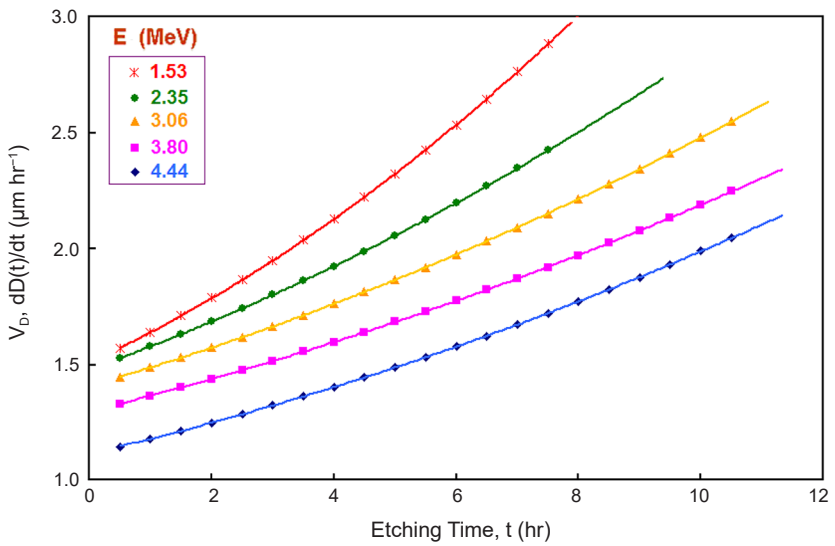

Figure 2: V_D as a function of etching time for different alpha particle energies in CR-39.

4.3 Bulk Etch Rate (V_B)

As mentioned before, the method of thickness difference was used to determine V_B of the detector. It was found that the removed layer thickness from the detector surface is linearly proportional to the etching time as shown in Figure 3. The computed value of V_B based on Equation 9 was found to be equal to 1.264 μm h^{-1} for the CR-39 detector etched under an aqueous 6.25 N solution of NaOH at 70°C. However, the obtained V_B value agrees with that found by Ahmed and Yu et al. where V_B were 1.45 μm h^{-1} and 1.2 μm h^{-1} respectively, and also it agrees with Ho et al. of V_B = 1.23 μm h^{-1} for the same detector under the same etching conditions.[17,19,31]

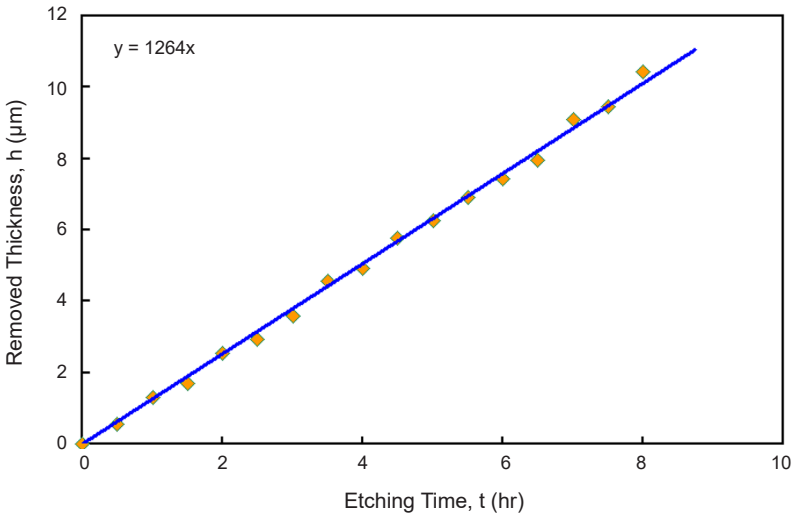

Figure 3: Thickness of the removed layer of CR-39 as a function of etching time.

4.4 Track Length Growth Rate

The track length growth rate (dL/dt) based on Equation 5 was calculated by using the data of $V_D(t)$ in Figure 2 and the value of V_B in Figure 3. Figure 4 shows that the dL/dt values are exponentially changing with the etching time, and their values at higher energies of alpha particles are greater than that of the lower ones. In general, the more increase in track opening diameter, the more increase in the (dL(t)/dt) is with advancing of the etching action even if the etching solution has passed the end of the particle trajectory (range) in the detector.

However, in contrast, it was found that the issue given in the previous discussion is no longer true at the depth more than the range of the particle in the detector, in the over-etched phase, and it is even far from the reality. It was known from the direct

measurements of the track length from the longitudinal images of the etched tracks carried out by other works that the dL(t)/dt, as well as the track length L(t), does not continue increasing as the track opening diameter increased with the advancing of the etching process.[5,8,15,17,18,26,32] This situation occurs particularly when the etching solution is passing the end of the particle range in the detector into the undamaged region beneath the range of the particle in the over-etched phase. Consequently, the residual range (R') at depths x > R will get negative values, which is unacceptable according to the Equation 8 where R' = R–x. In this case, the assumed boundary conditions are required to be applied in order to obtain the real variation of the dL(t)/dt as a function of the etching time, which coincides with that obtained from other studies based on direct measurement of the track lengths.

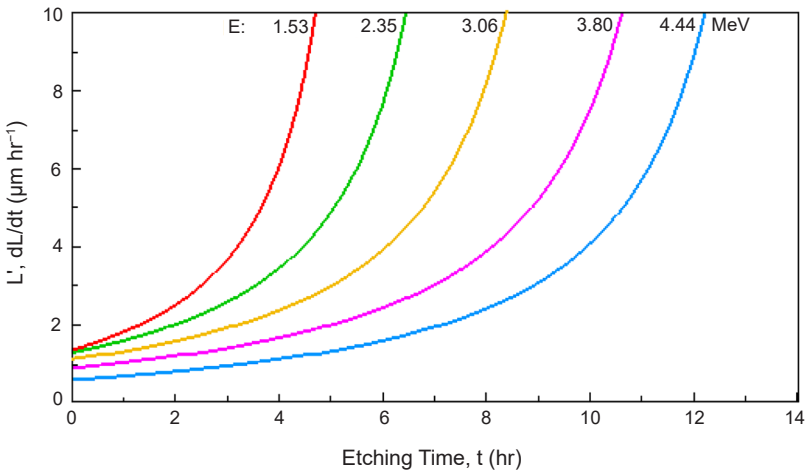

Figure 4: Relationship between dL/dt and the etching time for different alpha particle energies in CR-39.

By applying the boundary conditions (2 and 3), which assume that the dL/dt = 0 and L = L_{max} = constant when R' ≤ 0 and x ≥ R for all etching times more than the saturation time (t_{sat}), the curves in the Figure 4 were re-plotted and fitted again to extract the exact relationship between dL/dt and the etching time as shown in the Figure 5. The etching time is called the saturation time and denoted as t_{sat} when the track length is maximum (L_{max}) and the dL/dt is equal to zero, $(dL/dt)_o$.

Figure 5 shows that the dL(t)/dt is gradually increasing with the etching time and maximised, $(dL/dt)_{max}$, shortly before the track length reaches a constant value (saturation) at a point (or time) close to the end of the particle range in the detector. This point is the one where the energy loss rate of the alpha particles in the detector is maximised, and it coincides with the Bragg-peak of the stopping power curve. However, the result of dL(t)/dt in Figure 5 appeared in good

agreement with the results obtained by other studies based on direct measurements of the track lengths.[18] In contrast, the minimum or the zero-value $(dL/dt)_o$ occurs when the chemical etching reaches the end of the particle range in the detector where the track length is saturated and gets a maximum and constant value ($L = L_{max}$ = constant).

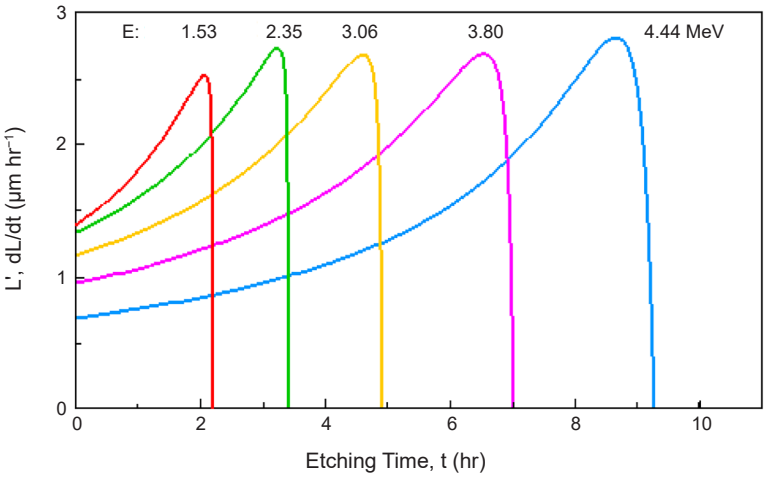

Figure 5: The real relationship between dL/dt and etching time for different alpha particle energies in CR-39 after applying the boundary conditions.

Thus, the values of $(dL/dt)_{max}$ and the etching times required to reach the maximum and zero-valued dL/dt (t_m and t_{sat}) for different alpha particle energies are shown in Table 1. It is seen from the table that the times t_m and t_{sat} depend on the energy of the alpha particles, while $(dL/dt)_{max}$ does not extremely dependent on it where its average value is about 2.692 μm h^{-1}. This result has appeared in good agreement with that found by Albelbasi, Ahmed and Azooz et al.[15–18]

Table 1: Maximum values and the times (t_m and t_{sat}) of the maximum$(dL/dt)_{max}$ and zero-valued $(dL/dt)_o$ of the dL/dt for different energies of alpha particles in CR-39.

E (MeV)	$(dL/dt)_{max}$ (mm h^{-1})	t_m (h)	t_{sat} (h)
1.53	2.52	2.08	2.25
2.32	2.74	3.24	3.46
3.06	2.69	4.63	4.93
3.80	2.70	6.54	6.90
4.44	2.81	8.70	9.22

Average $(dL/dt)_{max}$ = 2.692 μm h^{-1}

4.5 Track length

From Figure 4, the track length was determined by calculating the integration of dL(t)/dt with respect to the time using Equation 6 for various intervals from t = 0 to the experimentally considered and selected etching times (t) in each case of alpha particle energies. Again, by applying the boundary condition 2 where $L = L_{max}$ = constant (at saturation point), L'(=dL/dt) = 0, R' = 0 and R = x, the track lengths extracted from the integration were plotted as a function of the etching time as shown in Figure 6. It appears from the figure that the track length curve consists of two segments.[5,8,11,18,26,28] In the first segment, the track length develops exponentially and gets to maximum and constant value (saturation) when the etching solution reaches the end of the particle range in the detector where the particle range (damaged area) is completely etched. As a result, the track at this stage is called the etched-out track and it is conically shaped with a sharp tip at the end of the particle trajectory in the detector.

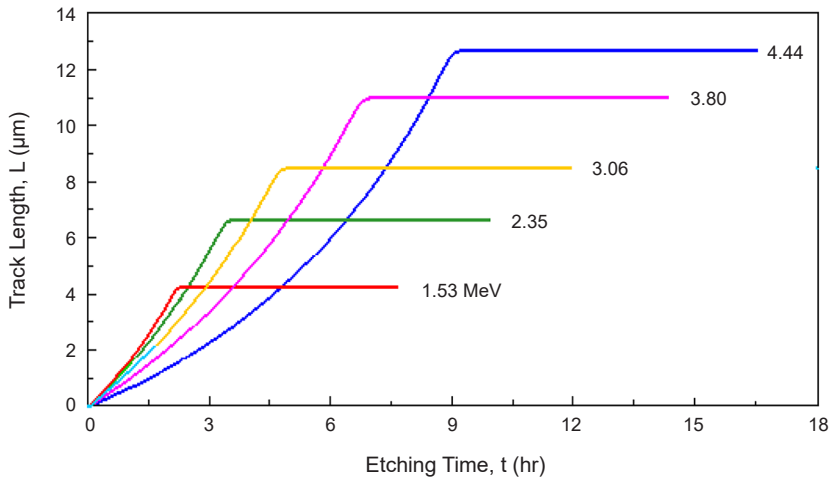

Figure 6: The real relationship between the track length and the etching time for different energies of the alpha particle in CR-39 after applying the boundary conditions.

In the second segment, the track length is saturated and continued within the steady (constant) value with the etching time. This part establishes when the etching solution passes the end of the particle range toward the sound region beneath the end of the particle range. When the track reaches this stage, named the over-etched phase, the tip of the conical track starts to become rounded and the track transforms progressively into a semi-spherical shape until reaching a total spherical form with the progressing of the etching process, and the track here is called the etch-pit.

With regards to the alpha particle energies, it is seen that the tracks at lower energies have a bigger size in the early times of the etching stages, and their lengths reach the constant or saturation faster than the tracks of high energies. Furthermore, the curves of the track length in Figure 6 have symmetric shapes but differ in the magnitude, and these results agree with those found elsewhere using the direct measurement of the track length of different alpha particle energies in PADC CR-39 detector.[11,17,18,25,26,33]

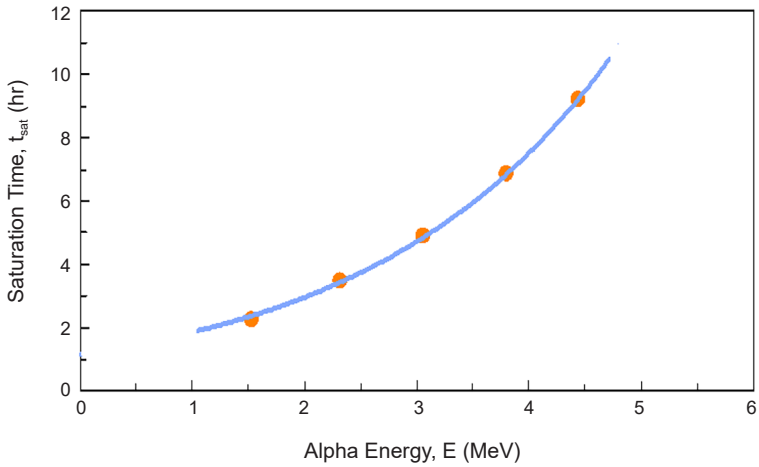

Figure 7: Saturation time as a function of the alpha particle energy in CR-39.

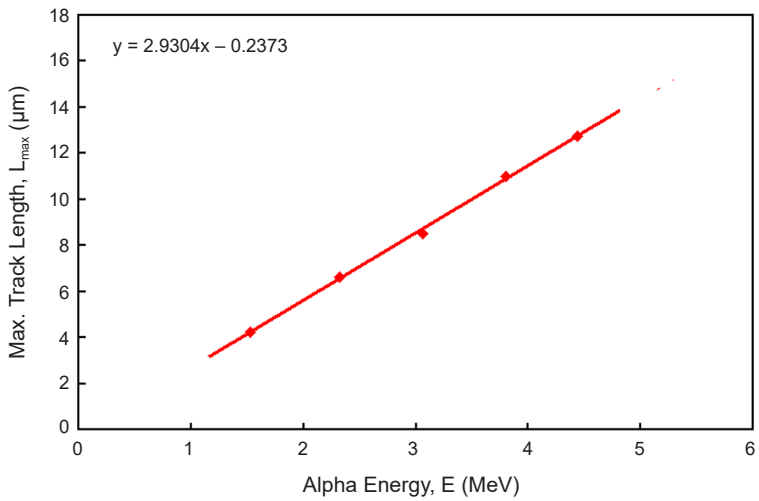

Figure 8: Maximum track length (saturation values) as a function of the alpha particle energy in CR-39.

Table 2 shows that L_{max} (or the saturation depth) and t_{sat} are essentially associated with the energy, and they occur at different depths from the detector surface. Accordingly, it is seen that t_{sat} is exponentially proportional to the energy of the alpha particles as shown in Figure 7, while L_{max} in Figure 8 is straightly proportional to the alpha particle energy. These results agree with those indicated by other works for alpha particles in CR-39, and furthermore, it agrees with Yamauchi et al. for alpha particle and ^{7}Li ion tracks in CR-39 in view of the direct measurement of the track lengths.[17,18,26,28,33] However, the small variance between the values of the saturation time (t_{sat}) in the Tables 1 and 2, that extracted from zero-valued $(dL/dt)_o$ points in the Figure 5 and L_{max} points in the Figure 6, is due to the fitting process of the curves in these figures.

Table 2: Maximum track length and the saturation time related to various alpha particle energies in CR-39.

E (MeV)	L_{max} (μm)	t_{sat} (h)
1.53	4.23	2.28
2.32	6.64	3.49
3.06	8.54	4.92
3.80	11.01	6.89
4.44	12.76	9.21

4.6 Track Etch Rate (V_T)

The development phases of the track's shape are mainly related to the V_T along the particle trajectory in the detector and how to change with the etching time (t) and the track depth (x).[11,24,34] Equation 3 was considered to calculate the V_T for all etching periods at various alpha particle energies. Again, by considering the boundary condition 3 and with regards to etching rates at $x > R$, the residual range of the particle gets a negative value (R' = -ve) and V_T equals to V_B. This situation begins from the point of saturation of the track length when the track etching enters the over-etched phase in the undamaged region. As indicated by the above assumption, the V_T data were plotted as a function of the etching time for the considered energies of the alpha particles as shown in Figure 9. The figure illustrates that the V_T is not constant during the etching process, but rather it changes and gets different maximum values at certain etching times based on the particle energies, and after then it rapidly drops to meet V_B where the etching passes the end of the particle range in the detector.

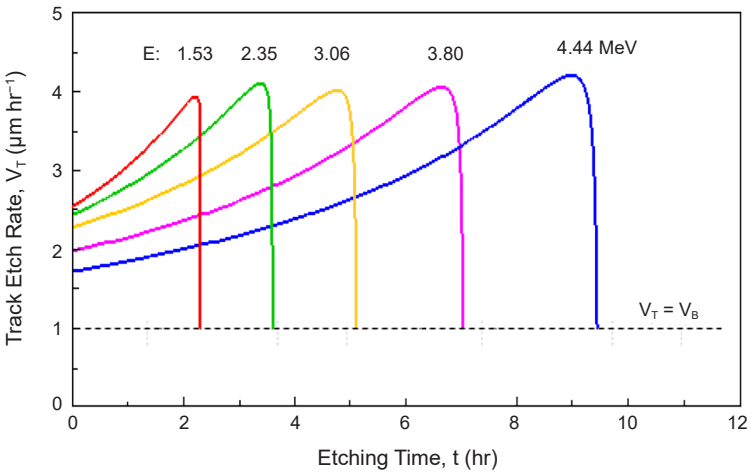

Figure 9: V_T as a function of the etching time for different alpha particle energies in CR-39 after applying the boundary conditions.

Table 3 lists the maximum values of the track etch rate (V_{Tmax}) and the time to access the maximum values (t_m). Here, the V_{Tmax} is roughly independent of the alpha particle energies. The table shows that the values of V_{Tmax} appear close together with an average value around 4.092 μm h^{-1}. This result is consistent with those extracted by using the direct measurement of the track (longitudinal depth) length within the range of our considered alpha particle energies as it was pointed by other works.[11,17,18]

It should be noted that the V_T has a maximum value (V_{Tmax}) at the Bragg-peak where alpha particles lose a large portion of the rest energy shortly before stopping. It can be observed that the V_{Tmax} value (Figure 9) occurs at the point where the dL/dt is maximised, i.e., $(dL/dt)_{max}$ (Figure 5). However, these results were consistent with other studies in computing V_T in alpha particle irradiated CR-39 with different energies using the track length measurement.[11,17,18,23,24,29]

By advancing the etching process for a short time after the maximum point, the alpha particle slows down significantly and then stops at the end of the range after losing the remaining portion of its energy. On the other hand, the track length lasts slightly increased during this period and reaches the maximum value (L_{max}) at the beginning point of the saturation, at the end of the particle range, where (dL/dt) gets to be distinctly zero.

Again, by analysing Table 3, it can be seen that the time of the V_{Tmax} (t_m) is exponentially increasing with the energy of the alpha particles. This time is exactly the same time of the $(dL/dt)_{max}$ as it is clear from the comparison of values of t_m

in the Tables 1 and 3. The presence of the minor differences between the two comparable times, which do not exceed 0.1 h in the most of the cases, is due to the fitting process of the curves in Figures 5 and 9.

Table 3: V_{Tmax} and the time to access to it for different alpha particle energies in CR-39.

E (MeV)	V_{Tmax} (μm h^{-1})	t_m (h)
1.53	3.96	2.16
2.32	4.13	3.35
3.06	4.04	4.71
3.80	4.09	6.58
4.44	4.24	8.90

Average V_{Tmax} = *4.092 μm* h^{-1}

The comparison between the t_m of the V_{Tmax} in Table 3 and t_{sat} of the L_{max} at saturation point or depth in Table 2 indicates that a short time lag exists between them which is between 0.18–0.31 h for alpha energies 1.53–4.44 MeV as shown in Figure 10. This short time here is the time of the equivalent distance, in the stopping power curve, that should be moved by the incident alpha particle from the point where the average energy loss per unit path length is a maximum (i.e., the Bragg-peak) to the point where the particle is ceased at the end of its range in the detector.

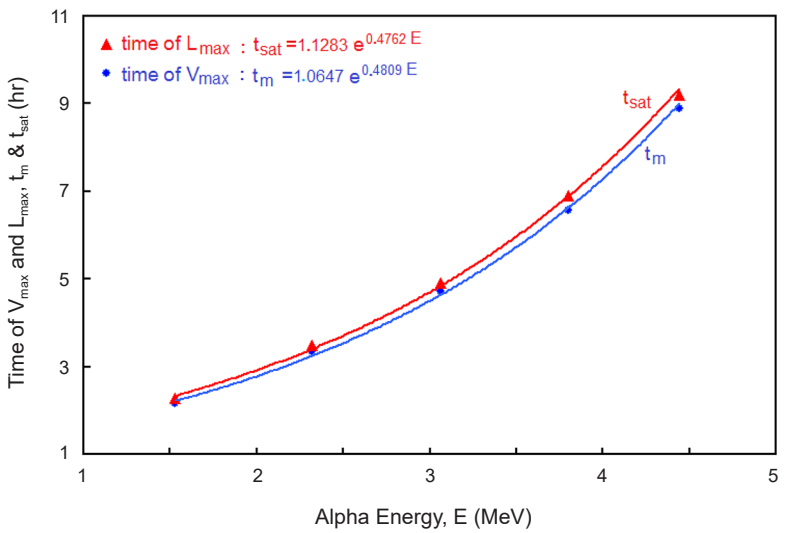

Figure 10: Comparison between the times (t_m) of V_{Tmax} (Table 3) and the times (t_{sat}) of maximum track length at saturation point (Table 2) in CR-39.

4.7 Etch Rate Ratio Function

The etch rate ratio or the response of the detector, V, is defined by two essential parameters; the V_T and the V_B as indicated by Equation 4. The ratio V is viewed as one of the imperative parameters to determine the behaviour of the track development and its shape advancement. Due to the dependence of V on the etching time and the track depth (x), it is necessary to plot V as a function of the residual range (R') to determine its real variation with the progress of the etching process.

To obtain the realistic behaviour of the V(R') using the method or the treatment proposed in this paper, the boundary condition 3 should be applied. This condition is associated with V_T where $V_T = V_B$ and V = 1 when the depth of the track extends to a point greater than the range of the particle in the detector (x > R), and the residual range gets distinctly negative values (R' = -ve) after the saturation point of the track length, in over-etched phase. So, considering this condition, the computed V values are adjusted to be equivalent to unity for all negative values of R', and after then the V data are re-plotted as a function of R' by using the form of V(R') function presented by Brun et al. for each considered alpha particle energy in this paper as shown in Figure 11.[35]

Figure 11 demonstrates that the V value increases with the advancing of the etching process and gets a maximum value V_{max} such as V_{Tmax} (see Figure 9) at the Bragg-peak.[23,24,29] Shortly after the maximum point, the V drops significantly and approaches the unity upon the arrival of the etching solution to the end of the particle range in the detector. This point represents the end of the primary phase of the track development, the conical phase, where $x \leq R$ and the track is completely etched-out. After crossing this point, the track development enters the second phase (x > R), the over-etched phase, where the etching of the sound area down the end of the particle range is started with rate V = 1 and $V_T = V_B$. The etching rate here lasts with the same value (scalar etching rate) in all directions as long as the etching is progressing in this region. Hence, the tip of the conically shaped track starts rounded and the track will convert into a semi-spherical shape with advancing of the etching process, and lastly to the spherical shape where the real track of the incident particle is terminated.

However, the result in Figure 11 which is based on the experimental measurements of the track diameters appeared in good agreement with that found by Azooz et al. based on the experimental measurements of the track length (or the track longitudinal depth).[18]

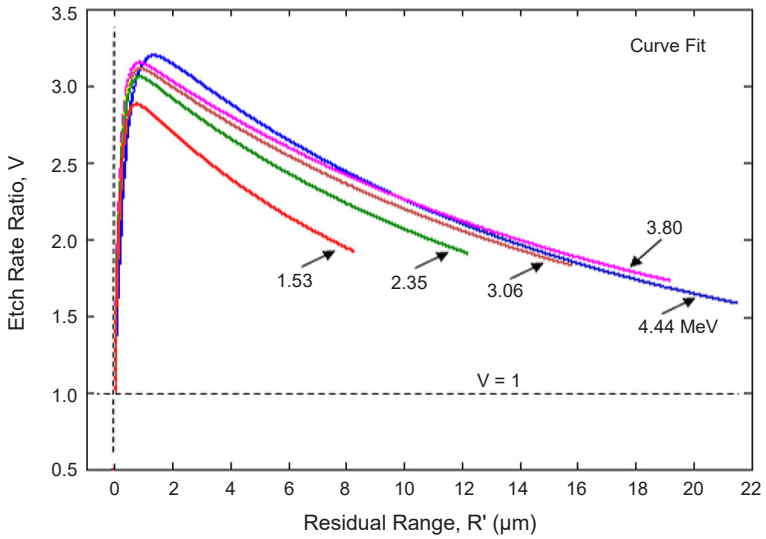

Figure 11: Etch rate ratio, V as a function of the alpha particle residual range in CR-39 after using the boundary conditions.

The peaks (V_{max}) in Figure 11 have indistinguishable shapes and approximately equal values, which are 3.17, 3.11, 3.08, 3.03 and 2.81 for alpha particle energies of 1.53 MeV, 2.32 MeV, 3.06 MeV, 3.80 MeV and 4.44 MeV, respectively. This indicates that V_{max} (as a V_{Tmax}) depends not so much on the energy of the alpha particles, and it has an average value about 3.04 as it is shown in Figure 12. The obtained result was consistent with that found by Nikezic and Yu, Ahmed and Azooz et al.[13,17,18]

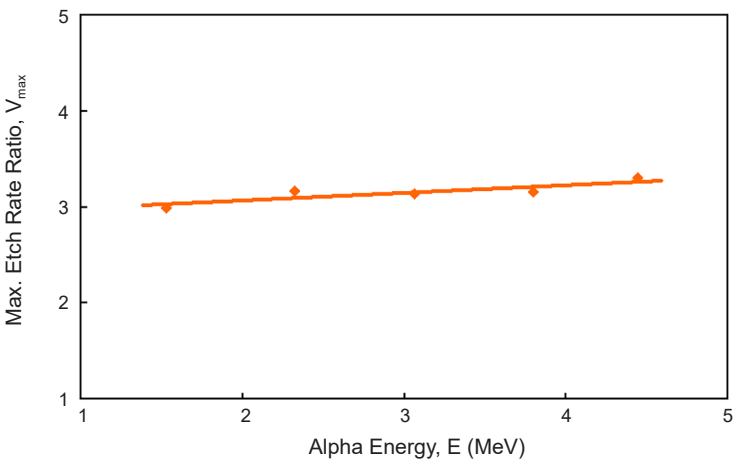

Figure 12: V_{max} verses alpha particle energies in CR-39.

4.8 Residual Range and the Maximum Track Length

Corresponding to Equation 8, it is noted that the residual range of the incident particle (R') is linearly proportional to the track depth (x) as long as the range of the incident particle (R) calculated from the Stopping and Range of Ions in Matter (SRIM) program is constant for a given energy. The range of the incident alpha particle can be computed from the results in Table 2 using the empirical relationship based on Equation 10:[18]

$$R = L_{max} + V_B t_{sat} \quad (10)$$

Table 4 illustrates the values of the alpha particle range for different energies in the CR-39 detector calculated by using both the empirical relationship (Equation 10) and the theoretical program SRIM.[36] A good agreement was found between the values of both calculations.

Table 4: Alpha particle range in CR-39 using both the Empirical Relationship and the theoretical program SRIM.[36]

E (MeV)	R (μm)	
	Calculated by Eq. 10	Calculated by SRIM
1.53	7.188	6.524
2.32	11.203	10.324
3.06	14.759	14.404
3.8	19.719	19.26
4.44	24.401	23.675

V_B = 1.264 μm h^{-1}

4.9 Fitting the Function V(R')

Fitting the data of the V(R') curves in Figure 11 for the considered etching times and alpha particle energies all at once is an imperative issue to obtain a single optimum curve independent of the particle energies. Therefore, the Brun et al. V(R') function presented in Equation 11 was used to perform the fitting process by Matlab curve fitting toolbox, and estimating the constants of A_1, A_2, B_1, B_2 and B_3 in accordance with our set of experimental data.[35] It should be noted that this function represents the second relationship presented in the Track-Test program for PADC CR-39 detector.[8]

$$V(R') = 1 + \exp(-A_1*R'+B_1) - \exp(-A_2*R'+B_2) + \exp(B_3) - \exp(B_1) \quad (11)$$

Figure 13 illustrates the optimum fitted curve of the function V(R') in CR-39 according to the direct measurement of the track diameters in the scope of alpha particle energies of 1.53–4.44 MeV under the assumed etching conditions. The constants of the fitted function V(R') were found equal to: $A_1 = 0.06271$ μm^{-1}, $A_2 = 3.321$ μm^{-1}, $B_1 = 0.742$, $B_2 = 0.7733$, $B_3 = 0.7756$, and the goodness of fit were SSE: 1.353, R-square: 0.9494, RMSE: 0.1141.

The style of the V(R') curve in Figure 13 is similar to the Bragg's ionising curve. The V(R') has a maximum value (peak) at a point close to the end of the particle range in the detector which is compatible with the Bragg-peak in the stopping power curve. In some ways, the V function is a reflection of some parameters for the primary interaction of the particle with the detector material. However, the maximum value of the fitted etch rate ratio function V_{max} appear equal to 3.0 with residual range R' = 1.32 μm. This distance represents the separation from the Bragg-peak to the end of the range of the alpha particle in the CR-39 detector.

In the same context, Ahmed has found that $V_{max} = 5.03$ at R' = 1.82 μm using Brun et al. function (Equation 11), as appeared in the Figure 14(a), while Albelbasi has found that $V_{max} = 3.8$ at R' = 2.0 μm using Green et al. function in the fitting process for different ranges of alpha particle energies in the CR-39 detector under the same etching circumstances as used here.[15,17,37] They have extracted their own particular constants of the function V(R') in accordance to their experimental data of the direct measurement of the track lengths. Moreover, the results also agreed with Nikezic and Yu for alpha particles in CR-39 using the Brun et al. V(R') function (Equation 11) where the V_{max} was 3.65 at R' = 2.65 as shown in Figure 14(b).[7]

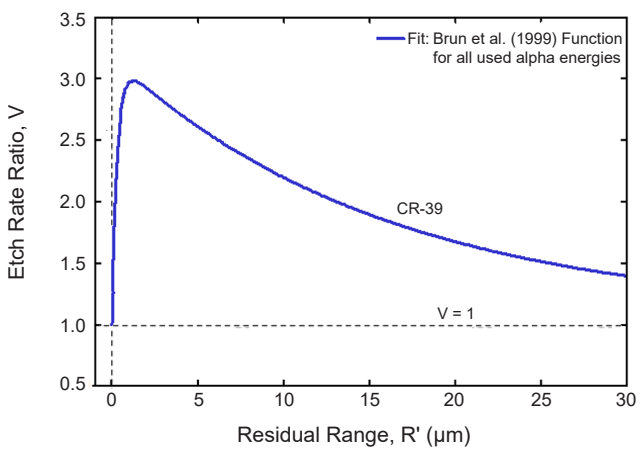

Figure 13: Fitted curve of the V(R') function for alpha-particle irradiated CR-39 detector for all considered energies in the present study using Equation 11; the Brun et al. function.[35]

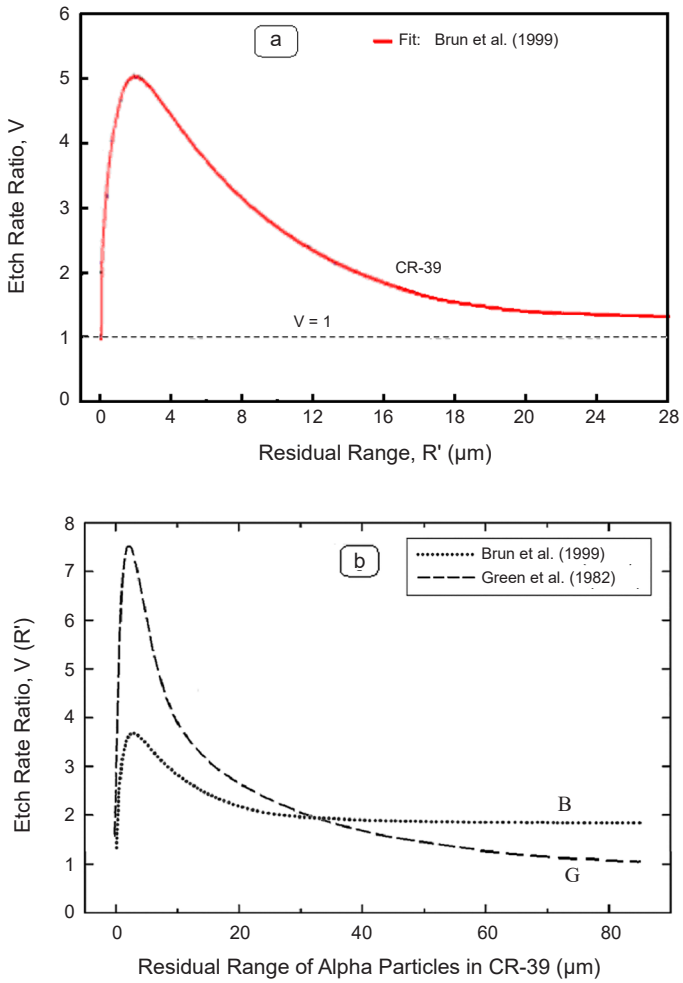

Figure 14: The fitted etch rate ratio function V(R') for alpha-particle irradiated CR-39 detector presented by (a) Ahmed[17] and (b) Nikezic and Yu.[7]

5. CONCLUSION

The diameter of the alpha particle tracks in PADC CR-39 detector appeared nonlinearly changes with the etching period. The nonlinear change results in V_D not to be constant, but it slightly varies and it gets different values with respect to the etching time for a single energy irradiation of the alpha particle in the detector. The new method or treatment assumed in this paper has been based on the concept of non-constancy of the V_D and using the experimental data of direct measurement of the track opening diameters.

Applying the new treatment and the modified equations required certain limitations or boundary conditions to compute the track parameters and its shape developing. These conditions were extracted from the experimental results and the calculations of the direct measurements of the longitudinal depth (or length) of the track profile. The method has succeeded in computing the track parameters such as the track length and depth, the residual range, the etching rates, the fitting of V(R') function and its constants A_1, A_2, B_1, B_2 and B_3 in CR-39. The extracted constants by this method can be easily used in Track-Test program to draw the track profiles and to determine the real variation of track parameters and the shape development in the CR-39 detector instead of the track imaging. However, the new treatment becomes more significant and useful for studying the profile and the shape development of the track in the nitrate cellulose detector LR115, in which the imaging of the etched track profiles is not possible.

Thus, the new treatment or method can be viewed as a straightforward and easy to apply and no need for complicated requirements and methodology compared with the methods based on track length measurements.

6. ACKNOWLEDGEMENTS

The author is indebted to the Physics Department, Mosul University, Iraq for supporting the present work. I would like to thank Prof. Dr. Laith A. Najam and Dr. Naseem S. Khidhir for their kind suggestions and for the many different ways they have contributed.

7. REFERENCES

1. Fews, A. P. & Henshaw, D. L. (1982). High-resolution alpha particle spectroscopy using CR-39 plastic track detector. *Nucl. Instr. Meth.*, 197, 517–529, https://doi.org/10.1016/0167-5087(82)90349-0.
2. Fromm, M., Chambaudet, A. & Membrey, F. (1988). Data bank for alpha particle tracks in CR39 with energies ranging from 0.5 to 5 MeV recording for various incident angles. *Nucl. Tracks Radiat. Meas.*, 15, 115–118, https://doi.org/10.1016/1359-0189(88)90112-4.
3. Nikezic, D. (2000). Three dimensional analytical determination of the track parameters. *Radiat. Meas.*, 32, 277–282, https://doi.org/10.1016/S1350-4487(00)00034-2.
4. Nikezic, D., Yu, K. N. & Kostic, D. (2003). Three-dimensional model of track growth: Comparison with other models. *Nucl. Tech. Radiat. Prot.*, 2, 24–30.

5. Nikezic, D. & Yu, K. N. (2003). Three-dimensional analytical determination of the track parameters: Over-etched tracks. *Radiat. Meas.*, 37, 39–45, https://doi.org/10.1016/S1350-4487(02)00129-4.
6. Dörschel, B. et al. (2003). 3D computation of the shape of etched tracks in CR–39 for oblique particle incidence and comparison with experimental results. *Radiat. Meas.*, 37, 563–571, https://doi.org/10.1016/S1350-4487(03)00243-9.
7. Nikezic, D. & Yu, K. N. (2004). Formation and growth of tracks in nuclear track materials. *Mater. Sci. Eng. R*, 46, 51–123, https://doi.org/10.1016/j.mser.2004.07.003.
8. Nikezic, D. & Yu, K. N. (2006). Computer program Track-Test for calculating parameters and plotting profiles for etch pits in nuclear track materials. *Comp. Phys. Comm.*, 174, 160–165, https://doi.org/10.1016/j.cpc.2005.09.011.
9. Nikezic, D. & Yu, K. N. (2008). Computer program TRACK_VISION for simulating optical appearance of etched tracks in CR-39 nuclear track detector. *Comp. Phys. Comm.*, 178, 591–595, https://doi.org/10.1016/j.cpc.2007.11.011.
10. Wertheim, D. et al. (2010). 3-D imaging of particle tracks in solid state nuclear track detector. *Nat. Haz. Earth Syst. Sci.*, 10, 1033–1036, https://doi.org/10.5194/nhess-10-1033-2010.
11. Azooz, A. A., Al-Nia'emi, S. H. & Al-Jubbori, M. A. (2012). A parameterization of nuclear track profiles in CR-39 detector. *Comp. Phys. Comm.*, 183, 2470–2479, https://doi.org/10.1016/j.cpc.2012.06.011.
12. Nikezic, D., Ivanovic, M. & Yu, K. N. (2016). A computer program TRACK-P for studying proton tracks in PADC detectors. *SoftwareX*, 5, 74–79, https://doi.org/10.1016/j.softx.2016.04.006.
13. Nikezic, D. & Yu, K. N. (2002). Profiles and parameters of tracks in the LR-115 detector irradiated with alpha energy. *Nucl. Instr. Meth. Phys. Res. B*, 196, 105–112, https://doi.org/10.1016/S0168-583X(02)01277-6.
14. Yip, C. W. Y. et al. (2006). Chemical etching characteristics for cellulose nitrate. *Mater. Chem. Phys.*, 95, 307–312, https://doi.org/10.1016/j.matchemphys.2005.06.024.
15. Albelbasi, S. O. R. (2007). Computation of etched track parameters and profiles for alpha particles in CR-39 and comparison with experimental results. MSc diss., University of Mosul, Iraq.
16. Hermsdorf, D. & Hungera, M. (2009). Determination of track etch rates from wall profiles of particle tracks etched in direct and reversed direction in PADC CR-39 SSNTDs. *Radiat. Meas.*, 44(9–10), 766–774, https://doi.org/10.1016/j.radmeas.2009.10.007.

17. Ahmed, H. A. (2010). Comparison of measured track profiles and parameters with the theoretical calculations of different models and the linear energy transfer of alpha particles in CR-39. MSc diss., University of Mosul, Iraq.
18. Azooz, A. A., Al-Nia'emi, S. H. & Al-Jubbori, M. A. (2012 b). Empirical parameterization of CR-39 longitudinal track depth. *Rad. Meas.*, 47, 67–72. https://doi.org/10.1016/j.radmeas.2011.10.015.
19. Yu, K. N. et al. (2004). Measurement of parameters of tracks in CR-39 detector from replicas. *Radiat. Prot. Dosimetry*, 111(1), 93–96, https://doi.org/10.1093/rpd/nch367.
20. Yu, K. N., Ng, F. M. F. & Nikezic, D. (2005). Measuring depths of sub-micron in a CR-39 detector from replicas using atomic force microscopy. *Radiat. Meas.*, 40, 380–383, https://doi.org/10.1016/j.radmeas.2005.03.011.
21. Dörschel, B. et al. (1997). Measurement of track parameters and etch rates in proton-irradiated CR–39 detectors and simulation of neutron dosimeter response. *Radiat. Prot. Dosim.*, 69(4), 267–274, https://doi.org/10.1093/oxfordjournals.rpd.a031913.
22. Tse, K. C. C., Nikezic, D. & Yu, K. N. (2008). Effect of UVC irradiation on alpha-particle track parameters in CR-39. *Radiat. Meas.*, 43, 98–101, https://doi.org/10.1016/j.radmeas.2008.03.029.
23. Vaginay, F. et al. (2001). 3-D confocal microscopy track analysis: A promising tool for determining CR-39 response function. *Radiat. Meas.*, 34, 123–127, https://doi.org/10.1016/S1350-4487(01)00136-6.
24. Fromm, M., Awad, M. & Ditlov, V. (2004). Many-hit model calculations for track etch rate in CR-39 SSNTD using confocal microscope data. *Nucl. Instr. Meth. Phys. Res. B*, 226, 565–574, https://doi.org/10.1016/j.nimb.2004.07.004.
25. Al-Nia'emi, S. H. S. (2015). Effects of chemical solution temperature on the bulk etch rate of the detector CR-39. *Jord. J. Phys.*, 8(1), 49–55.
26. Dörschel, B. et al. (1998). Track parameters and etch rates in alpha-irradiated CR-39 detectors used for dosimeter response calculation. *Radiat. Prot. Dosim.*, 78(3), 205–212, https://doi.org/10.1093/oxfordjournals.rpd.a032353.
27. Durrani, S. A. & Bull, R. K. (1987). *Solid state nuclear track detection: Principles, methods, and applications*. Oxford: Pergamon Press.
28. Yamauchi, T. et al. (2001). Inter-comparison of geometrical track parameters and depth dependent track etch rates measured for Li-7 ions in two types of CR–39. *Radiat. Meas.*, 34, 37–43, https://doi.org/10.1016/S1350-4487(01)00117-2.
29. Ditlov, V. A. et al. (2005). The Bragg-peak studies in CR-39 SSNTD on the basis of many-hit model for track etch rates. *Radiat. Meas.*, 40, 249–254, https://doi.org/10.1016/j.radmeas.2005.03.009.

30. Roussetski, A. S. et al. (2005). Correct identification of energetic alpha and proton tracks in experiments on CR-39 charged particle detection during hydrogen desorption from Pd/PdO:Hx heterostructure. Paper presented at the Condensed Matter Nuclear Science Proceedings of the 12th International Conference on Cold Fusion, ICCF 2005, https://doi.org/10.1142/9789812772985_0032.
31. Ho, J. P. Y. et al. (2003). Differentiation between tracks and damages in SSNTD under the atomic force microscope. *Radiat. Meas.*, 36, 155–159, https://doi.org/10.1016/S1350-4487(03)00114-8.
32. Ng, F. M. F. et al. (2007). Determination of alpha-particle track depths in CR-39 detector from their cross-sections and replica heights. *Nucl. Instr. Meth. Phys. Res. B*, 263, 266–270, https://doi.org/10.1016/j.nimb.2007.04.147.
33. Al-Hubeaty, Y. Y. K (2013). Modification of modeling the profiles of alpha particles tracks in the nuclear detector CR-39 according to the chemical etchant concentration. MSc diss., University of Mosul, Iraq.
34. Dörschel, B., Hartmann, H. & Kadner, K. (1996). Variations of the track etch rates along the alpha particle trajectories in two types of CR–39. *Radiat. Meas.*, 26(1), 51–57, https://doi.org/10.1016/1350-4487(95)00270-7.
35. Brun, C. et al. (1999). Intercomparative study of the detection characteristics of the CR–39 SSNID for light ions: Present status of the Besancon-Dresden approaches. *Radiat. Meas.*, 31, 89–98. https://doi.org/10.1016/S1350-4487(99)00102-X.
36. Ziegler, J. F., Ziegler, M. D. & Biersack, J. P. (2008). The stopping and range of ions in matter. Retrieved from http://www.srim.org/ on 15 July 2017.
37. Green, P. G. et al. (1982). A study of bulk-etch rates and track-etch rates in CR-39. *Nucl. Instr. Meth*., 2037, 551–559, https://doi.org/10.1016/0167-5087(82)90673-1.